

Searching for blue in the dark

Jessie de Kruijf,^{1,2,*} Eleonora Vanzan,^{1,2,†} Kimberly K. Boddy,^{3,‡} Alvisè Raccanelli,^{1,2,4,§} and Nicola Bartolo^{1,2,4,¶}

¹*Dipartimento di Fisica Galileo Galilei, Università di Padova, I-35131 Padova, Italy*

²*INFN Sezione di Padova, I-35131 Padova, Italy*

³*Texas Center for Cosmology and Astroparticle Physics, Weinberg Institute,
Department of Physics, The University of Texas at Austin, Austin, TX 78712, USA*

⁴*INAF-Osservatorio Astronomico di Padova, Italy*

The primordial power spectrum of curvature perturbations has been well-measured on large scales but remains fairly unconstrained at smaller scales, where significant deviations from Λ CDM may occur. Measurements of 21-cm intensity mapping in the dark ages promise to access very small scales that have yet to be probed, extending beyond the reach of CMB and galaxy surveys. In this paper, we investigate how small-scale power-law enhancements—or blue tilts—of the primordial power spectrum affect the 21-cm power spectrum. We consider generic enhancements due to curvature modes, isocurvature modes, and runnings of the spectral tilt. We present forecasts for Earth- and lunar-based instruments to detect a blue-tilted primordial spectrum. We find that an Earth-based instrument capable of reaching the dark ages could detect any enhancements of power on nearly all the scales it can observe, which depends on the baseline of the interferometer. The smallest scales observed by such an instrument can only detect a very strong enhancement. However, an instrument on the far side of the Moon of the same size would be able to probe shallower slopes with higher precision. We forecast results for instruments with 100 km (3000 km) baselines and find that they can probe up to scales of order $k_{\text{max}} \sim 8 \text{ Mpc}^{-1}$ ($k_{\text{max}} \sim 250 \text{ Mpc}^{-1}$), thereby providing invaluable information on exotic physics and testing inflationary models on scales not otherwise accessible.

I. INTRODUCTION

The power spectrum of primordial perturbations describes the initial conditions of the Universe and thus of structure formation. It is well-characterized by curvature perturbations ζ on relatively scales from roughly 10^{-4} to 1 Mpc^{-1} , by measurements of cosmic microwave background (CMB) anisotropies and large-scale structure (LSS) [1–7].

Previous work has constrained the primordial power spectrum on smaller scales using the abundance of ultracompact minihalos [8], the distribution of stars in an ultra-faint dwarf galaxy [9], spectral distortions of the CMB [10, 11], and the high-redshift UV galaxy luminosity function [12, 13]. However, these methods can have large astrophysical uncertainties, preventing them from achieving the same level of sensitivity and robustness as the constraints from CMB anisotropies and LSS. Possible future CMB experiments, such as PIXIE [14] and CMB-HD [15], could reach scales up to $k \sim 10 \text{ Mpc}^{-1}$.

Probing the primordial power spectrum on small scales could be the key to discovering new physics [16, 17]. Many exotic physics models generate an increase (or blue tilt) of the small-scale power spectrum, such as nonstandard inflationary scenarios [18–29], gravitational particle production of dark matter [30–35], axions [36, 37], quantum decoherence during inflation [38], and bouncing cosmolo-

gies [39, 40]. Such blue-tilted primordial (or matter) power spectra have been investigated using CMB/LSS [41], spectral distortions [42], dark matter substructure [8, 9, 43, 44], quasar light curves [45], Lyman- α forest [46], and Milky Way satellite velocities [47, 48]. There have also been forecasts for constraining blue tilts with Euclid and MegaMapper [49], as well as for SKAO using 21-cm line-intensity-mapping (LIM) at relatively low redshifts ($z < 20$) [50].

In this work, we consider the sensitivity that future 21-cm fluctuation measurements from the dark ages have to enhancements of small-scale power, with respect to Λ CDM. The main benefit of measuring the 21-cm power spectrum during the dark ages [51–57], which spans the redshift range $30 \lesssim z \lesssim 200$, is that there is no astrophysical contamination, since the first stars have not yet formed; thus, we can more directly probe early Universe cosmology. Moreover, fluctuations are not affected by Silk damping [58] and therefore remain undamped down to the baryon Jeans scale $k_J \sim 300 \text{ Mpc}^{-1}$. As a result, we can access modes at much smaller scales with 21-cm LIM, compared to the CMB.

There are several proposals for low-frequency interferometers that would be able to detect the dark ages 21-cm signal. Most are lunar-based experiments [59–66], as well as a lunar-orbiting CubeSat [67]. It was also the aim of several Earth-based instruments to observe the dark ages [68–72]. While the current designs are not yet capable of reaching such high redshifts, future versions of them potentially could. We consider the sensitivity to enhancements of small-scale power for a few hypothetical instruments, both Earth- and lunar-based.

Previous studies have investigated how changes to the matter power spectrum affect the 21-cm signal [73–82]; most of them consider a suppression or enhancement

*Electronic address: jessiearnoldus.dekruijf@phd.unipd.it

†Electronic address: eleonora.vanzan@phd.unipd.it

‡Electronic address: kboddy@physics.utexas.edu

§Electronic address: alvise.raccanelli.1@unipd.it

¶Electronic address: nicola.bartolo@pd.infn.it

of small-scale structure for particular models. We take an agnostic approach by considering generic power-law enhancements of the primordial power spectrum due to a small-scale enhancement of curvature modes, the addition of uncorrelated cold dark matter isocurvature modes to the standard Λ CDM curvature modes, and a running of the spectral tilt. We find that an Earth-based instrument can already probe most power spectra increases on the observable scales, while a lunar-based instrument of the same size can probe shallower slopes and obtain a higher accuracy. When increasing the size of the instrument on the Moon, one can probe a much larger range of scales, allowing revolutionary and stringent tests of exotic physics and inflationary models.

This paper is organized as follows. In Section II we introduce different blue-tilted power spectra considered in this work. In Section III we give a brief overview of 21-cm LIM from the dark ages. In Section IV we describe our methods for measuring the blue-tilted power spectrum and provide the instrument specifications we use for our forecasts. In Section V we show the results of our forecasts. We summarize our findings and conclude in Section VI.

II. BLUE-TILTED PRIMORDIAL POWER SPECTRUM

Within the standard Λ CDM scenario, the dimensionless primordial curvature power spectrum

$$\Delta_{\zeta}^2(k) = A_s \left(\frac{k}{k_0} \right)^{n_s - 1} \quad (1)$$

is characterized by a tilt n_s and amplitude A_s at the pivot scale k_0 . Measurements of CMB anisotropy from the *Planck* satellite, in conjunction with LSS data, show that this power spectrum is nearly scale-invariant and red-tilted (i.e., decreases with k) with $n_s = 0.9649 \pm 0.0084$ (95% CL, *Planck* TT, TE, EE + lowE + lensing), and has an amplitude given by $\ln(10^{10} A_s) = 3.044 \pm 0.028$ (95% CL, *Planck* TT, TE, EE + lowE + lensing) at $k_0 = 0.05 \text{ Mpc}^{-1}$ [1]. These values are compatible with the simplest prediction of single-field, slow-roll inflation.

While the CMB and LSS set robust and stringent constraints on large scales, its behavior is largely unconstrained on small scales, allowing for the possibility of physics beyond Λ CDM to enter at $k > 1 - 10 \text{ Mpc}^{-1}$.

Small-scale enhancements arise from a variety of early Universe physics, such as inflationary scenarios [18–29], gravitational particle production of dark matter [30–35], axions [36, 37], quantum decoherence during inflation [38], and bouncing cosmologies [39, 40]. These scenarios produce blue-tilted enhancements in the total primordial power spectrum $\Delta^2(k)$, either by directly increasing curvature power spectrum at small scales or by generating small-scale cold dark matter isocurvature.

In this section, we consider a primordial power spectrum that becomes blue-tilted (i.e., increases with k) at scales smaller than 1 Mpc^{-1} . We study enhancements of three

different types: a curvature power spectrum with a broken power law; a blue-tilted cold dark matter isocurvature power spectrum; and the running of the spectral tilt, $n_s(k)$, which is a necessary feature of a primordial power spectrum that transitions from a red tilt at large scales to a blue tilt at small scales.

A. Enhanced curvature power spectrum

We start by considering primordial blue-tilted curvature power spectra at small scales, which can be produced by e.g. [18–23, 25–29, 38, 39]. The primordial spectrum may possess additional features, such as a turnover that produces a bump at some large value of k . Since such features are model-dependent, we do not account for them. However, we impose a threshold of $\Delta_{\zeta}^2(k) \leq 0.01$, forcing the power spectrum to remain constant at arbitrarily large k . The presence of the threshold has no significant impact on our analyses.¹

To investigate small-scale enhancements in a model-independent manner, we adopt a simple broken-power-law parameterization of the dimensionless primordial curvature power spectrum:

$$\Delta_{\zeta}^2(k) = \begin{cases} A_s \left(\frac{k}{k_0} \right)^{n_s - 1} & k < k_b \\ A_b \left(\frac{k}{k_b} \right)^{n_b} & k > k_b, \end{cases} \quad (2)$$

where k_b is the scale where the power spectrum breaks and begins to increase as a power law with index n_b . The amplitude A_b of the small-scale power is defined at the scale k_b , and continuity demands $A_b = A_s (k_b/k_0)^{n_s - 1}$. Assuming $k_b \gtrsim 1 \text{ Mpc}^{-1}$, $\Delta_{\zeta}^2(k)$ coincides with Eq. (1) for $k < k_b$ and thus remains within the limits set by CMB and LSS on large scales. On smaller scales $k > k_b$, we allow for new physics to produce a blue-tilted spectrum. Figure 1 illustrates the power-law break in Eq. (2) for various values of k_b and n_b .

The power-law scaling for $k > k_b$ in Eq. (2) can be mapped to various models. For example, for tilted hybrid inflation [27], the spectral index and the amplitude of the power spectrum can be mapped to the effective mass of the inflaton field and the value of the field at the moment when perturbations that have momentum k at the end of inflation were produced. Another example is quantum decoherence during inflation [38]. The evolution of inflationary curvature perturbations can be modified due to the interaction with other degrees of freedom present in the early Universe. This interaction leads to quantum decoherence, and in various cases to a blue-tilted

¹ There are cases in which the threshold is imposed at scales relevant to our analyses. However, these situations occur in the signal-dominated regime, so our projections based on signal-to-noise ratios remain insensitive to the threshold.

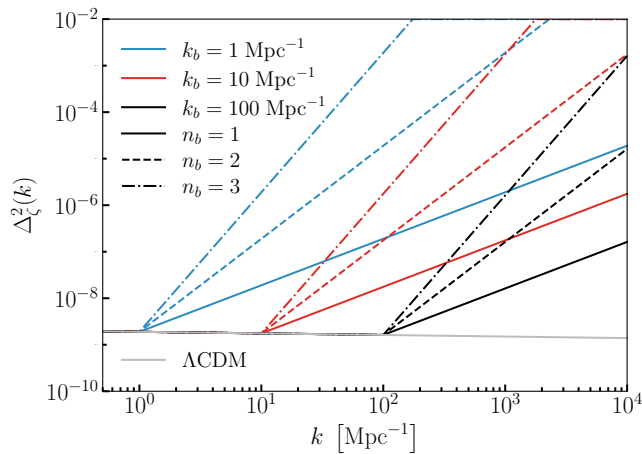


Figure 1: Dimensionless primordial curvature power spectrum. We show the power-law break from the Λ CDM case (solid gray) at various values of k_b , with a blue-tilted enhancement for $k > k_b$ for various values of the power-law index n_b .

correction of the power spectrum on scales considered in this work. The time dependence and strength of the interaction between the perturbations and other degrees of freedom determine n_b and k_b .

B. Enhanced dark matter isocurvature power spectrum

A different class of small-scale enhancements arises from the production of isocurvature modes [24, 30–36, 36, 37, 50, 83–91]. We assume that adiabatic modes give rise to the dimensionless primordial curvature power spectrum in Eq. (1), and the isocurvature modes produce a dimensionless primordial isocurvature power spectrum

$$\Delta_{\mathcal{S}_{\text{cdm}}}^2(k) = A_{\text{iso}} \left(\frac{k}{k_0} \right)^{n_{\text{iso}}-1}, \quad (3)$$

with a tilt n_{iso} and an amplitude A_{iso} at the *Planck* pivot scale k_0 . Although the adiabatic and isocurvature modes are generically correlated, we assume for simplicity that they have no cross-correlation power, such that the total dimensionless primordial power spectrum is

$$\Delta^2(k) = \Delta_{\zeta}^2(k) + \Delta_{\mathcal{S}_{\text{cdm}}}^2(k), \quad (4)$$

as demonstrated in Fig. 2. For all scenarios considered in this work, we have checked explicitly that the amplitudes are consistent with constraints from *Planck* [7]. Similar to the curvature case, we impose a threshold of $\Delta^2(k) \leq 0.01$.

A blue-tilted isocurvature power spectrum can arise, for example, from the QCD axion [37, 89, 90, 92], which produces an isocurvature spectral index of $1 < n_{\text{iso}} \leq 4$. The bounds on the isocurvature parameters can be translated to a bound on the inflationary energy scale H_I [93, 94]. A similar translation can be done in the

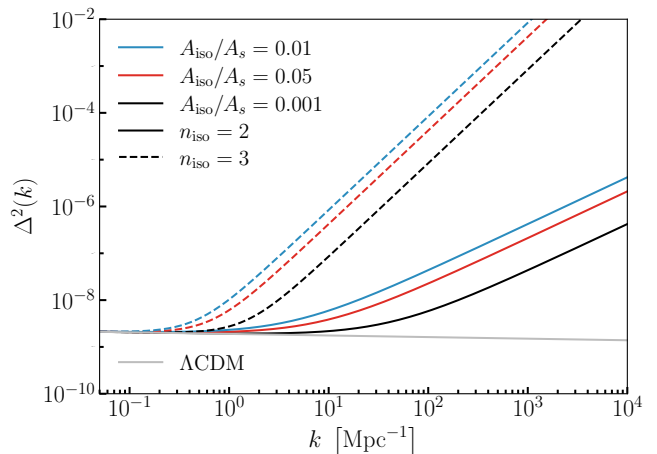


Figure 2: Total dimensionless primordial power spectrum $\Delta^2(k)$, for curvature and cold dark matter isocurvature modes. We show the increase of the power spectrum, along with the Λ CDM case (solid gray), due to isocurvature modes for various values of n_{iso} and A_{iso}/A_s .

context of ultralight axions [95], for which H_I depends on A_{iso}/A_s and the fraction of dark matter that ultralight axions constitute.

Alternatively, a blue tilt with $n_{\text{iso}} = 4$ can be generated by particle production mechanisms with a finite correlation length. The resulting isocurvature power spectrum vanishes on scales smaller than a cutoff scale determined by causality, and only white noise is left on these smaller scales. Examples of such mechanisms are post-inflationary dark matter production [96, 97], vector dark matter [35, 98], and PQ-breaking during inflation with subsequent axion production [99].

C. Running parameters

The parameterization in Eq. (2) is meant to describe the main features of the primordial spectrum; however, if there is a transition from the decreasing to the increasing behavior as a function of k , this transition would be described by the first and higher order derivatives of the spectrum. We parameterize the primordial power spectrum in this case as [100]

$$\Delta_{\zeta}^2(k) = A_s \left(\frac{k}{k_0} \right)^{n_s-1} \times \exp \left[\frac{1}{2} \alpha_s \log^2 \left(\frac{k}{k_0} \right) + \frac{1}{6} \beta_s \log^3 \left(\frac{k}{k_0} \right) \right], \quad (5)$$

where

$$\alpha_s = \frac{dn_s}{d \log k}, \quad \beta_s = \frac{d\alpha_s}{d \log k}, \quad (6)$$

are the first and second running parameters of the tilt, respectively [100, 101]. *Planck* 2018 data constrains the

running parameters to be $\alpha_s = 0.013 \pm 0.012$ and $\beta_s = 0.022 \pm 0.012$ (at the pivot scale $k = 0.05 \text{ Mpc}^{-1}$) [1, 7, 102].

Standard single-field slow-roll inflation predicts $\alpha_s \sim (1 - n_s)^2 \sim \mathcal{O}(\epsilon^2, \eta^2) \sim 10^{-3}$ and $\beta_s \sim (1 - n_s)^3 \sim \mathcal{O}(\epsilon^3, \eta^3) \sim 10^{-5}$ [78, 100, 103, 104]. Therefore, high precision constraints on the running parameters could either confirm or rule out this inflationary scenario and permit tests of other inflationary models that predict a running, such as multifield [105], and warm inflation [106].

Note that this parameterization is only valid for small deviations from the scale-invariant case and is thus not appropriate for the large enhancements studied in Section II A. We focus on the region of k in which the power spectrum begins to transition to becoming blue tilted, and thus the parameterization is valid.

III. 21-CM INTENSITY MAPPING DURING THE DARK AGES

In this section we describe the main observable of interest: the intensity mapping signal of 21-cm neutral hydrogen. We provide a brief review of key concepts for 21-cm LIM from the dark ages, before the formation of the first stars, which occurs around $z \sim 30$ in ΛCDM .² For more details, we refer the reader to Refs. [53, 107–110] for 21-cm LIM, Refs. [51, 52, 54, 111–113] for specific application to the dark ages, and Refs. [114, 115] for recent reviews on LIM.

Post recombination, the Universe is filled with neutral hydrogen gas clouds. The CMB photons act as a backlight, scattering on neutral hydrogen atoms and exciting the 21-cm hyperfine transition between the singlet and the triplet state. During the dark ages, the temperature of the gas is lower than that of the CMB, and there is a net absorption of CMB photons of wavelength $\lambda_{21} \approx 21 \text{ cm}$ with corresponding frequency $\nu_{21} \approx 1420 \text{ MHz}$. The remaining CMB photons at the transition frequency are redshifted as the Universe expands. Therefore, observing a deficit of CMB photons at a given frequency identifies a unique redshift slice for the absorption process, thereby enabling tomographic analyses.

The observed quantity for the 21-cm signal is the brightness temperature contrast with respect to CMB [82],

$$T_{21} = \frac{T_s - T_{\text{CMB}}}{1+z} (1 - e^{-\tau}) \approx \tau \frac{T_s - T_{\text{CMB}}}{1+z}, \quad (7)$$

where we have assumed the optically thin limit in which the optical depth $\tau \ll 1$. The spin temperature T_s is

defined by the ratio of abundances of neutral hydrogen in the triplet state n_1 and in the singlet state n_0 :

$$\frac{n_1}{n_0} \equiv 3e^{-E_{10}/T_s} \approx 3 \left(1 - \frac{E_{10}}{T_s}\right), \quad (8)$$

where $E_{10} \approx 5.9 \mu\text{eV}$ is the energy difference between the two states. Collisions of neutral hydrogen with other atoms and electrons drive $T_s \rightarrow T_{\text{gas}}$, while radiative transitions involving absorption of and emission to the radio background drive $T_s \rightarrow T_{\text{CMB}}$. A nonzero T_{21} is possible only after T_{gas} decouples from T_{CMB} at redshift $z \sim 200$. Frequent collisions keep T_s coupled to T_{gas} , allowing for a net absorption of 21-cm CMB photons by neutral hydrogen. Around $z \sim 100$, the expansion of the Universe dilutes the gas sufficiently to render collisions inefficient, and T_s tends toward T_{CMB} .

The Sobolev optical depth [116] is

$$\tau = \frac{3}{32\pi} \frac{E_{10}}{T_s} x_{\text{HI}} n_H \lambda_{21}^3 \frac{A_{10}}{H(z) + (1+z)\partial_r v}, \quad (9)$$

where x_{HI} is the fraction of neutral hydrogen, n_H is the number density of hydrogen, $A_{10} \approx 2.85 \times 10^{-15} \text{ s}^{-1}$ is the spontaneous decay rate of the spin-flip transition, $H(z)$ is the Hubble parameter, and $\partial_r v$ is the line-of-sight gradient of the peculiar velocity of the gas. During the dark ages, $\tau \ll 1$, and the approximation in Eq. (7) is valid.

The brightness temperature is a function of the local hydrogen density and the gas temperature, and it can be parameterized as [82]

$$T_{21} = \bar{T}_{21} (1 + \delta_v) + c_b \delta_b + c_T \delta_{T_{\text{gas}}}, \quad (10)$$

where $\delta_b = \delta n_b / \bar{n}_b \simeq \delta_H$ up to negligible corrections, $\delta_{T_{\text{gas}}} = \delta T_{\text{gas}} / T_{\text{gas}}$, and $\delta_v = -(1+z)\partial_r v / H(z)$. The coefficients $c_{b,T}$ are functions of redshift only; the mean brightness temperature \bar{T}_{21} is defined by setting all perturbations to zero. Following Ref. [117], we neglect fluctuations in the gas temperature and in the neutral hydrogen fraction to write the 21-cm brightness temperature fluctuations as

$$\delta T_{21}(\mathbf{x}, z) \simeq \alpha(z) \delta_b(\mathbf{x}, z) + \bar{T}_{21}(z) \delta_v(\mathbf{x}, z), \quad (11)$$

where $\alpha(z) = dT_{21}/d\delta_b$.

We expand the angular dependence of the brightness fluctuations in the basis of spherical harmonics,

$$\delta T_{21}(\mathbf{x}, z) = \sum_{\ell m} a_{\ell m}(z) Y_{\ell m}(\hat{\mathbf{x}}), \quad (12)$$

and write the angular power spectrum of 21-cm fluctuations as

$$\langle a_{\ell m}(z) a_{\ell' m'}(z) \rangle = C_\ell(z) \delta_{\ell\ell'} \delta_{mm'}. \quad (13)$$

By combining Eq. (11) with the continuity equation, we can directly relate the 21-cm angular power spectrum to the matter power spectrum $P_m(k)$ [82, 117, 118]:

$$C_\ell(z) = \frac{2}{\pi} \int_0^\infty k^2 dk \mathcal{T}_\ell(k, z)^2 P_m(k), \quad (14)$$

² We note that enhancements of small-scale structure should lead to advanced star formation. Studying the onset of cosmic dawn is beyond the scope of this work, and we use $z = 30$ as a convenient reference redshift for our forecasts.

with

$$\mathcal{T}_\ell(k, z) = \int_0^\infty dx W_\nu(x) \left[\alpha(z) j_\ell(kx) - \bar{T}_{21}(z) \frac{\partial^2 j_\ell(kx)}{\partial(kx)^2} \right], \quad (15)$$

where $W_\nu(x)$ is a window function and $j_\ell(kx)$ is the spherical Bessel function of the first kind.

The matter power spectrum is linked to the primordial curvature power spectrum via

$$P_m(k, z) = \sum_X D_X(z)^2 \frac{2\pi^2}{k^3} \Delta_X^2(k) T_{m,X}(k)^2, \quad (16)$$

where $X = \{\zeta, \mathcal{S}_{\text{cdm}}\}$ represents the initial condition, and we assume the adiabatic and cold dark matter isocurvature modes are uncorrelated. We use CLASS [119] to compute the linear growth factor $D_X(z)$ and the matter transfer function $T_{m,X}(k)$. In the Λ CDM case, the power spectrum is still linear for the scales and redshifts we probe. In the cases where the primordial power spectrum reaches values above 10^{-3} at the scales of interest, the resulting matter power spectrum could become non-linear. For our results, the majority of the sensitivity is near the ℓ_{max} value (see Section V for more details), and we do not expect our conclusions to be affected by assuming the matter power spectrum is still linear; a careful investigation of this issue is left for future work.

The window function $W_\nu(x)$ in Eq. (15) accounts for the finite spectral resolution of the instrument. We model the window function as a tophat, centered at the radial distance $x(z)$ corresponding to the targeted redshifted frequency $\nu = \nu_0/(1+z)$. The width of the window

$$\Delta x = \frac{(1+z)^2}{\nu_0 H(z)} B \quad (17)$$

depends on the frequency bandwidth B .

IV. METHODOLOGY

In this section we describe our procedure for forecasting the sensitivity of future 21-cm LIM experiments to enhancements of small-scale power. We consider three proposed future instruments as examples: one Earth-based instrument, inspired by the Square Kilometre Array Observatory (SKAO), and two lunar instruments with different sensitivities.

For our forecasts, we take Λ CDM as a reference model, using the *Planck* 2018 best fit values [1] for the fiducial cosmological parameters: $\{\omega_b = 0.02238, \omega_c = 0.1201, h = 0.6781, n_s = 0.96605, \ln 10^{10} A_s = 3.0448\}$.

A. Forecasting setup

We estimate the detectability of a given set of parameters controlling the deviation from Λ CDM of the primordial power spectrum by calculating the signal-to-noise

ratio (SNR) as [120]

$$\text{SNR}^2 \approx f_{\text{sky}} \sum_z \sum_\ell \left(\frac{C_\ell^{\text{blue}}(z) - C_\ell^{\Lambda\text{CDM}}(z)}{\sigma_\ell} \right)^2, \quad (18)$$

where C_ℓ^{blue} and $C_\ell^{\Lambda\text{CDM}}$ are the blue-tilted and Λ CDM 21-cm angular power spectra, respectively, f_{sky} is the fraction of the sky observed, and the variance is

$$\sigma_\ell^2 = \frac{2(C_\ell^{\Lambda\text{CDM}} + C_\ell^{\text{noise}})^2}{(2\ell + 1)}. \quad (19)$$

The sum in Eq. (18) runs over all redshift bins and over all multipoles up to the maximum observable multipole

$$\ell_{\text{max}}(z) = 2\pi \frac{D_{\text{base}}}{\lambda(z)}, \quad (20)$$

where D_{base} the baseline of a given instrument, and $\lambda(z) = \lambda_{21}(1+z)$ is the redshifted 21-cm wavelength.

We model the noise power spectrum as [121]

$$C_\ell^{\text{noise}}(z) = (2\pi)^3 \frac{T_{\text{sys}}^2(\nu)}{B t_{\text{obs}} f_{\text{cover}}^2} \left(\frac{1}{\ell_{\text{max}}(z)} \right)^2, \quad (21)$$

where t_{obs} is the total time of observation, and f_{cover} is the coverage fraction (i.e., the fraction of the array area that is covered by antennas). We take the system temperature to be the synchrotron temperature of the observed sky [121]:

$$T_{\text{sys}}(\nu) = 180 \left(\frac{180 \text{ MHz}}{\nu} \right)^{2.6}. \quad (22)$$

We assume that the redshift bins are independent, which is a good approximation provided that the correlation length in frequency is smaller than the bandwidth of the instrument. We define the radial correlation length ξ_r as the radial separation, beyond which the cross-correlation between two redshift slices is less than 1/2 of the power spectrum [122]. The corresponding correlation length in frequency is

$$\xi_\nu = \frac{d\nu}{dz} \frac{dz}{dr} \xi_r \approx 1 \text{ MHz} \left(\frac{51}{1+z} \right)^{1/2} \left(\frac{\xi_r}{60 \text{ Mpc}} \right). \quad (23)$$

We take linearly spaced bins in frequency, which we convert into redshift bins, and verify that ξ_ν is smaller than the bandwidth B of the instrument. We neglect cross-correlations between different redshift bins, since they are expected to be negligible for 21-cm LIM measurements [123].

For the case of running of the spectral tilt, we perform a Fisher matrix analysis [124–133], since we have a specific model with fiducial values for the running parameters (α_s, β_s); whereas for the blue-tilted curvature and isocurvature scenarios, we use the SNR to investigate which values of $\{k_b, n_s\}$ or $\{A_{\text{iso}}, n_{\text{iso}}\}$ we can test. The Fisher approach approximates the likelihood around its maximum as a

Gaussian and returns the smallest possible error on the parameter, namely the one set by the Cramer-Rao bound. The Fisher information matrix is

$$F_{\alpha\beta} = f_{\text{sky}} \sum_z \sum_{\ell} \sigma_{\ell}^{-2} \frac{\partial C_{\ell}}{\partial \vartheta_{\alpha}} \frac{\partial C_{\ell}}{\partial \vartheta_{\beta}}, \quad (24)$$

where $\vartheta_{\alpha,\beta}$ represent our running parameters, and the sums run over all multipoles up to ℓ_{max} and over all redshift bins, assuming there is no overlap in the amount of information contained in each bin.

B. Instruments

There are several proposals for low-frequency interferometers that would be able to detect the redshifted 21-cm signal from the dark ages. Most proposals are for lunar-based experiments, see e.g., [59–66, 134], including lunar-orbiting CubeSats [67]; more proposals are being developed for both lunar- and space-based interferometers [135]. These experiments are generally lunar-based, because the frequency of the redshifted signal from the end of the dark ages lies at the edge of where the Earth’s ionosphere becomes opaque [136, 137]. Moreover, the far side of the Moon should be completely radio quiet and stable [138], making it an ideal place for such an instrument.

There is an open debate on how well we will be able to model the signal and actually observe the end of the dark ages from the (Earth) ground. Several Earth-based instruments had planned to observe the dark ages [68–72], but this possibility is still uncertain; therefore, in this work we also consider an Earth-based instrument, assuming it will observe the very end of the dark ages, which we take to be at redshift $z = 30$.

In order to keep our findings as general as possible, we consider three surveys, the details of which are presented in Table I. The instruments are a future Earth-based instrument—an advanced version of the SKAO, which we refer to as SKAO-like, limited to $z = 30$ —and two possible configurations of a lunar radio array (LRA) on the far side of the Moon. We refer to the lunar instruments as LRAI and LRAII; we consider a baseline of 100 km for the former, while the latter has a baseline that spans nearly the diameter of the Moon to demonstrate the maximal capabilities of a lunar array.

For the instruments considered in this work, the predicted (Λ CDM) power spectrum and related uncertainties are shown in Fig. 3 for $z = 30$ (top) and $z = 100$ (bottom). The theoretical prediction for $C_{\ell}^{\Lambda\text{CDM}}$ is shown in gray for reference. The largest multipole observable is directly related to the baseline, while the magnitude of the error bars is mostly influenced by the signal and the f_{cover} .

	SKAO-like	LRAI	LRAII
B [MHz]	2	2	2
D_{base} [km]	100	100	3000
f_{cover}	0.2	0.5	0.75
t_{obs} [years]	10	10	10
f_{sky}	0.75	0.75	0.75

Table I: Instrument specifications. For each configuration, we list the assumed bandwidth in frequency B , baseline D_{base} , fraction of the instrument’s total area that is covered by antennas f_{cover} , observation time in years t_{obs} , and sky coverage fraction f_{sky} .

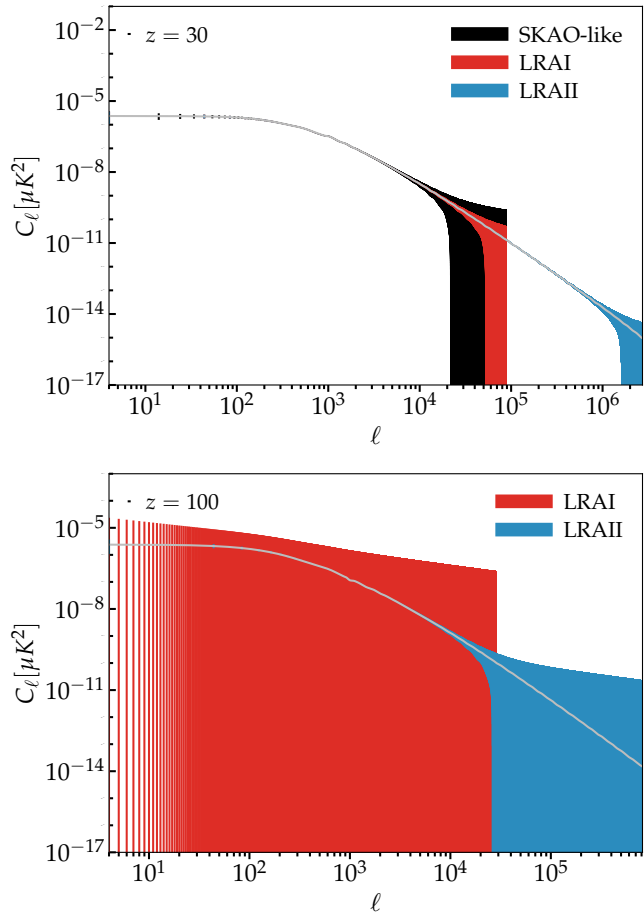


Figure 3: Angular power spectrum of 21-cm brightness temperature fluctuations at $z = 30$ (top panel) and $z = 100$ (bottom panel), with error bars for the instruments listed in Table I. The theoretical prediction for $C_{\ell}^{\Lambda\text{CDM}}$ is shown in gray for reference. The sharp cutoff at high multipoles corresponds to the maximum observable multipole.

V. RESULTS

Here we present our forecasted constraints on the models presented in Section II, using the methodology of Section IV A for the instruments of Section IV B.

A. Enhanced curvature power spectrum

We start by showing results for the parameterization in Eq. (2). In Fig. 4 we show the SNR for the detection of deviations from Λ CDM, as a function of the cutoff scale and slope $\{k_b, n_b\}$, for each instrument considered in this work. In the k range that is accessible to a given instrument, virtually any blue tilts would be easily detected with a high SNR. We expect this result, given the error bars shown in Fig. 3. Importantly, the baseline of the interferometer is a key feature for testing small-scale enhancements of the power spectrum. This point is also illustrated in Fig. 5, where we show how the SNR changes as a function of k_b for specific values of $n_b = 2, 3, 4$.

The highest value of k_b that can be probed is nearly identical to the highest k measured by the instrument, $k_{\max} = \ell_{\max} \times \chi(z)$, where ℓ_{\max} is given in Eq. (20) and $\chi(z)$ is the comoving distance. At $z = 30$, $k_{\max} \sim 8 \text{ Mpc}^{-1}$ for the small instruments (SKAO-like, LRAI), while $k_{\max} \sim 230 \text{ Mpc}^{-1}$ for the larger instrument (LRAII). Only for the lowest values of n_b and the highest k_b is the signal indistinguishable from the noise.

B. Enhanced dark matter isocurvature power spectrum

We now consider cold dark matter isocurvature modes that produce a blue-tilted isocurvature primordial power spectrum, given by Eq. (3). Figure 6 shows the SNR for the detection of isocurvature modes, as a function of the amplitude ratio A_{iso}/A_s and the spectral tilt n_{iso} , for each instrument considered in this work. The largest value we show for A_{iso}/A_s coincides with the upper bound from *Planck* [7]. An Earth-based instrument tapping into the dark ages can improve on the *Planck* constraints by about an order of magnitude, depending on the spectral index. The smaller lunar array, LRAI, would significantly increase the significance of such constraints, while the larger LRAII could improve the constraints by two orders of magnitude for very low value of n_{iso} and several orders more for higher tilts.

The sensitivity of 21-cm dark ages measurements would be better than that for future galaxy surveys. A large scale structure survey like Euclid allows, at best, to detect ($A_{\text{iso}}/A_s = 0.09, n_{\text{iso}} = 3$), while using an idealized version of MegaMapper could detect ($A_{\text{iso}}/A_s = 0.015, n_{\text{iso}} = 3; A_{\text{iso}}/A_s = 0.002, n_{\text{iso}} = 4$) [49].

C. Running parameters

We perform a Fisher forecast on the standard cosmological parameters $\{\omega_b, \omega_c, h, n_s, \ln 10^{10} A_s\}$, plus the running parameters $\{\alpha_s, \beta_s\}$. For fiducial values we take those of single-field slow-roll (SFSR) inflation: $\{\alpha_s, \beta_s\} = \{10^{-3}, 10^{-5}\}$ [100, 102]. We then perform two analyses:

	SKAO-like	LRAI	LRAII
α_s , varying cosmology	1.3×10^{-2}	1.3×10^{-3}	1.1×10^{-4}
β_s , varying cosmology	3.7×10^{-3}	5.1×10^{-4}	2.1×10^{-5}
α_s , fixed cosmology	1.3×10^{-3}	2.0×10^{-4}	3.5×10^{-6}
β_s , fixed cosmology	1.5×10^{-3}	2.0×10^{-4}	2.0×10^{-6}

Table II: Results from Fisher analyses for the first and second running parameters of the spectral index, α_s and β_s , respectively. We provide the 1σ errors with varying cosmological parameters (first two rows) and fixed cosmological parameters (bottom two rows), to be compared with *Planck* 2018 ($\simeq 0.01$ for both parameters). The fiducial values for the running parameters are taken to be the standard SFSR $\{\alpha_s, \beta_s\} = \{10^{-3}, 10^{-5}\}$.

one varying all the parameters above and one fixing cosmological ones to their *Planck* 2018 best fit values [1].

Table II shows predicted constraints for different instruments, indicating that the small lunar instrument, LRAI, could potentially test SFSR inflation through measurements of the α_s parameter, while the uncertainty on β_s would be too large. On the other hand, with the LRAII configuration, there could be a several sigma detection of (or a robust challenge to) α_s for the SFSR scenario. LRAII would also have the sensitivity to start probing β_s for SFSR. As a point of comparison, the uncertainties from *Planck* 2018 data are $\sigma \simeq 0.012$ for both parameters.

In the case where we vary cosmological parameters (first two rows in Table II), an SKAO-like experiment would be competitive with *Planck* for α_s and improve by an order of magnitude for β_s . Both lunar array cases would improve by 1 or more orders of magnitude over current CMB constraints, with LRAII being able to test the SFSR inflation scenario.

We also perform the Fisher analysis, fixing the standard Λ CDM parameter to demonstrate what the 21-cm experiments could achieve in principle. Additionally, by the time a lunar array would be built, it is possible that very strong prior could be placed on the cosmological parameters from future precision CMB experiments. In this case, an Earth-based instrument could start testing the SFSR scenario with α_s . Lunar arrays could measure α_s with extreme precision, while LRAII is needed to probe SFSR with β_s . With the aid of future very precise priors, 21-cm IM surveys may be able to put inflationary models under strong scrutiny.

As a point of comparison, Ref. [78] has forecasts for the spectral running parameters for future CMB and LSS experiments. While an Earth-based interferometer would be competitive with future CMB measurements, it would not provide strong improvements. The lunar arrays, however, would be more sensitive than future CMB+galaxy surveys, especially for the β_s parameter, for which the improvement could be orders of magnitude.

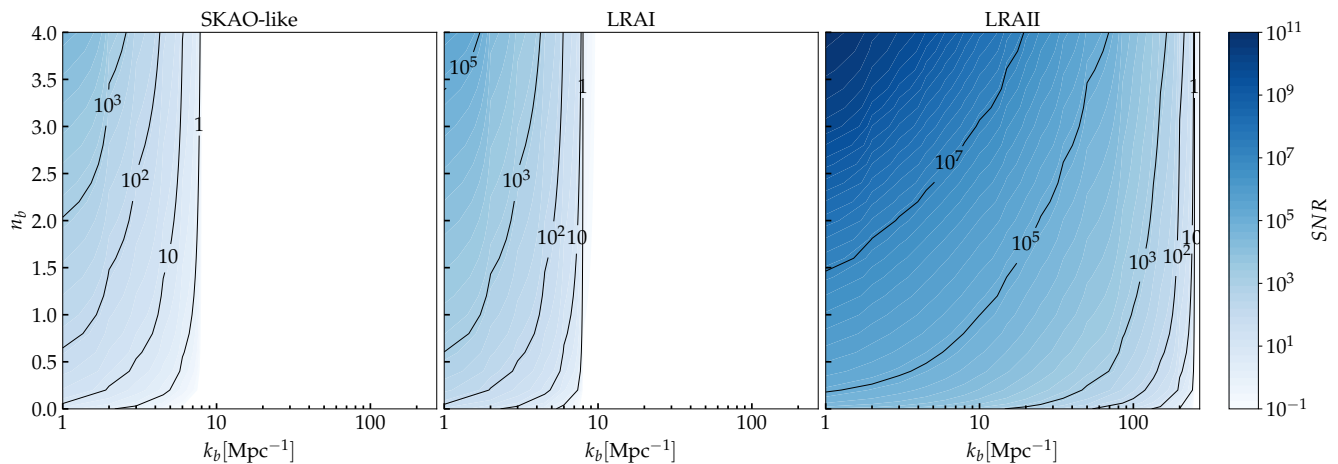


Figure 4: SNR of the blue-tilted deviation from Λ CDM for each of the instruments listed in Table I, shown for varying values of k_b and n_b . The white regions are those for which $\text{SNR} < 1$ and the instrument would have no sensitivity. The contour lines indicate several specific values of the SNR.

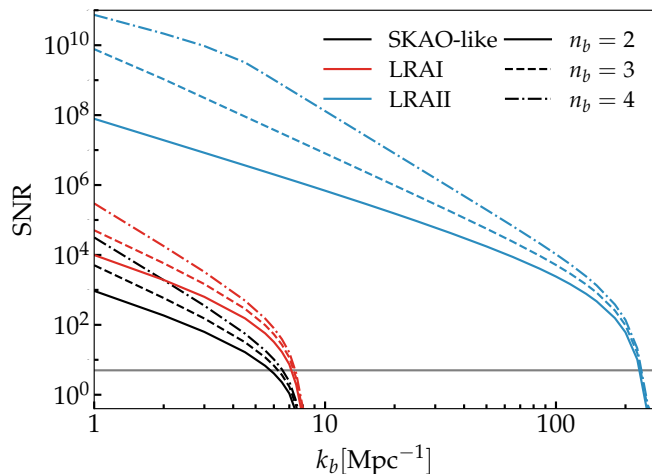


Figure 5: SNR of the blue-tilted deviation from Λ CDM for each of the instruments listed in Table I, shown as a function of k_b , for $n_b = 2, 3, 4$. We indicate $\text{SNR} = 5$ with a gray horizontal line for reference.

VI. CONCLUSIONS

The primordial power spectrum is well-constrained by CMB and LSS data to be almost scale-invariant (and slightly red-tilted) at large scales. Several new-physics and dark matter models can imprint small-scale deviations from Λ CDM and are still largely unconstrained. Many of these models induce an increase of power at smaller scales, producing a blue-tilted power spectrum.

In this work we investigate how future 21-cm intensity mapping interferometers targeting the dark ages can set limits on the enhancement of the power spectrum at small scales. We consider three example instruments: a future Earth-based experiment that could detect the end

of the dark ages (SKAO-like), and two radio arrays on the far side of the Moon (LRAI, LRAII). LRAI is similar to an SKAO extension but on the Moon; LRAII covers almost the entirety of the Moon's far side with radio antennas, as proof of principle for what can be achieved. For each instrument, we determine the signal-to-noise ratio for detecting a blue-tilted primordial power spectrum that arises from an enhancement of small-scale curvature modes and cold dark matter isocurvature modes.

For enhanced curvature modes, the most important instrumental feature is the baseline of the interferometer, which translates into the maximum multipole that the instrument can probe. We find that any blueness of the spectrum is detectable, as long as the growth starts within the probed multipole range. Thus, while the significance of the detection would be higher for a small lunar array, there would be not much difference from an Earth-based instrument with the same baseline. We analyze instruments with baselines of 100 km and 3000 km, which translates into detecting any blue-tilted deviation that occurs at scales larger than $k \sim 8 \text{ Mpc}^{-1}$ and $k \sim 230 \text{ Mpc}^{-1}$, respectively.

For small-scale enhancements from cold dark matter isocurvature modes, even just an Earth-based instrument would have greater sensitivity to a blue tilt than *Planck* or future galaxy surveys. Lunar arrays would further increase the significance of detection and, in the case of the LRAII, improve upon *Planck* constraints by several orders of magnitude.

Finally, we perform a Fisher analysis to forecast constraints on the running of the spectral tilt. Our results show that, while a Earth-based instrument can be competitive with current and near-future CMB experiments, lunar arrays could improve such constraints by one or more orders of magnitude, for both running parameters, depending on the priors we choose for the standard Λ CDM parameters. The larger LRAII could, even with no exter-

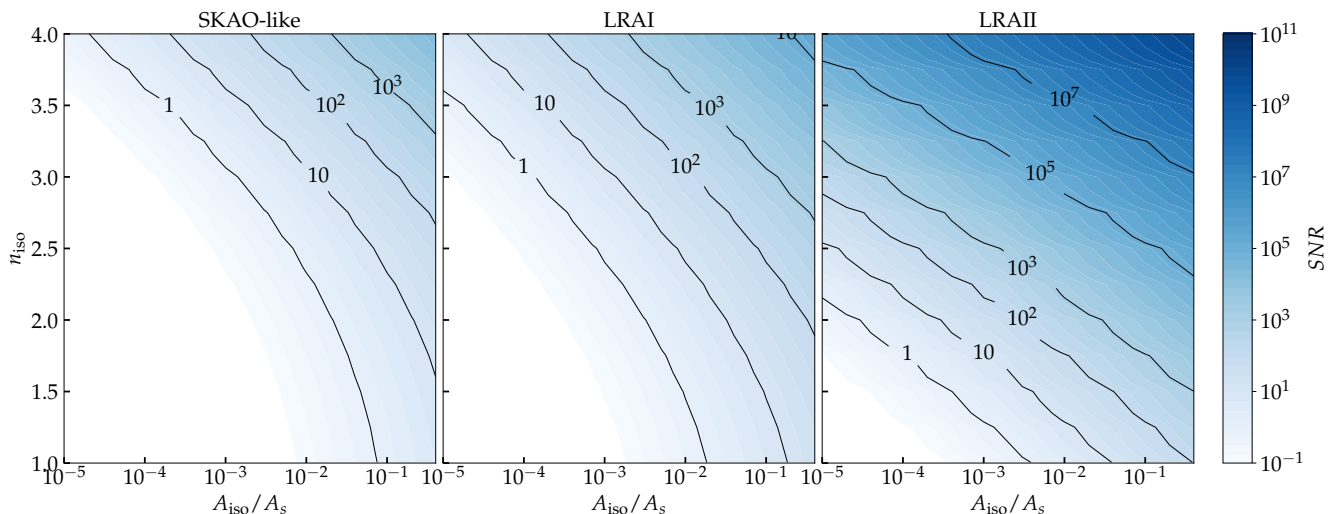


Figure 6: SNR for detecting blue-tilted cold dark matter isocurvature spectra, for each of the instruments listed in Table I, shown for varying values of A_{iso}/A_s and n_{iso} . The white regions are those for which $\text{SNR} < 1$ and the instrument would have no sensitivity. The contour lines indicate several specific values of the SNR.

nal priors, not only set very stringent constraints on the running parameters, but also probe the expected values for standard single-field slow-roll inflation.

In conclusion, interferometers capable of measuring the 21-cm signal from the cosmic dark ages would be able to detect blue spectra that could originate from several extensions to the standard cosmological and particle physics models. While we have focused on the scale and slope of the power spectrum increase, we note that these parameters can be mapped to specific inflationary and particle models. Given the range of scales that can be probed by such instruments, they could provide invaluable and otherwise unobtainable information on exotic physics and test inflationary models to unprecedented precision.

Acknowledgments

AR thanks the University of Texas, Austin, for the hospitality during the initial stages of this work. KB

thanks the University of Padova for the hospitality during the intermediate stages of this work. We thank Mustafa Amin, Nicola Bellomo, Andrew Long, and Julian Muñoz for useful discussions.

KB acknowledges support from the National Science Foundation (NSF) under Grant No. PHY-2112884 and acknowledges the “Dark Matter Theory, Simulation, and Analysis in the Era of Large Surveys” workshop and the Kavli Institute for Theoretical Physics (KITP) for the hospitality and support under NSF Grant No. PHY-2309135. AR acknowledges funding from the Italian Ministry of University and Research (MIUR) through the “Dipartimenti di eccellenza” project “Science of the Universe”.

-
- [1] N. Aghanim et al. (Planck), *Astron. Astrophys.* **641**, A6 (2020), [Erratum: *Astron. Astrophys.* 652, C4 (2021)], 1807.06209.
 - [2] A. Kalaja et al., *JCAP* **10**, 031 (2019), 1908.03596.
 - [3] M. M. Ivanov, M. Simonović, and M. Zaldarriaga, *JCAP* **05**, 042 (2020), 1909.05277.
 - [4] O. H. E. Philcox and M. M. Ivanov, *Phys. Rev. D* **105**, 043517 (2022), 2112.04515.
 - [5] M. M. Ivanov, *Phys. Rev. D* **104**, 103514 (2021), 2106.12580.
 - [6] D. Collaboration (2024), 2404.03002.
 - [7] Y. Akrami et al. (Planck), *Astron. Astrophys.* **641**, A10 (2020), 1807.06211.
 - [8] T. Bringmann, P. Scott, and Y. Akrami, *Phys. Rev. D* **85**, 125027 (2012), 1110.2484.
 - [9] P. W. Graham and H. Ramani, *Constraints on dark matter from dynamical heating of stars in ultrafaint dwarfs. part 2: Substructure and the primordial power spectrum* (2024), 2404.01378.
 - [10] J. Silk, *Annals of the New York Academy of Sciences* **375**, 188 (1981).
 - [11] J. Chluba et al., *Experimental Astronomy* **51**, 1515 (2021), 1909.01593.
 - [12] N. Sabti, J. B. Muñoz, and D. Blas, *The Astrophysical Journal Letters* **928**, L20 (2022), ISSN 2041-8213, 2110.13161, URL <http://dx.doi.org/10.3847/>

- 2041-8213/ac5e9c.
- [13] S. Yoshiura, M. Oguri, K. Takahashi, and T. Takahashi, *Physical Review D* **102** (2020), ISSN 2470-0029, 2007.14695, URL <http://dx.doi.org/10.1103/PhysRevD.102.083515>.
- [14] A. Kogut et al., *The primordial inflation explorer (pixie): Mission design and science goals* (2024), 2405.20403.
- [15] H. Collaboration, *Snowmass2021 cmb-hd white paper* (2022), 2203.05728, URL <https://arxiv.org/abs/2203.05728>.
- [16] K. Bechtol et al., in *Snowmass 2021* (2022), 2203.07354.
- [17] K. K. Boddy et al., *JHEAp* **35**, 112 (2022), 2203.06380.
- [18] J. Martin and R. H. Brandenberger, *Phys. Rev. D* **63**, 123501 (2001), hep-th/0005209.
- [19] J.-O. Gong and M. Sasaki, *JCAP* **2011**, 028 (2011), 1010.3405.
- [20] C. Germani and T. Prokopec, *Physics of the Dark Universe* **18**, 6 (2017), 1706.04226.
- [21] J. M. Ezquiaga, J. García-Bellido, and E. Ruiz Morales, *Physics Letters B* **776**, 345 (2018), 1705.04861.
- [22] G. Ballesteros, J. Rey, M. Taoso, and A. Urbano, *JCAP* **2020**, 025 (2020), 2001.08220.
- [23] S. S. Mishra and V. Sahni, *JCAP* **2020**, 007 (2020), 1911.00057.
- [24] M. Braglia et al., *JCAP* **2020**, 001 (2020), 2005.02895.
- [25] X. Wang, Y.-l. Zhang, and M. Sasaki (2024), 2404.02492.
- [26] S. Mollerach, S. Matarrese, and F. Lucchin, *Phys. Rev. D* **50**, 4835 (1994), astro-ph/9309054.
- [27] J. García-Bellido and A. Linde, *Physics Letters B* **398**, 18–22 (1997), ISSN 0370-2693, URL [http://dx.doi.org/10.1016/S0370-2693\(97\)00211-6](http://dx.doi.org/10.1016/S0370-2693(97)00211-6).
- [28] J. D. Barrow and A. R. Liddle, *Physical Review D* **47**, R5219–R5223 (1993), ISSN 0556-2821, URL <http://dx.doi.org/10.1103/PhysRevD.47.R5219>.
- [29] G. A. Palma, S. Sypsas, and C. Zenteno, *Physical Review Letters* **125** (2020), ISSN 1079-7114, URL <http://dx.doi.org/10.1103/PhysRevLett.125.121301>.
- [30] D. J. H. Chung, E. W. Kolb, A. Riotto, and L. Senatore, *Phys. Rev. D* **72**, 023511 (2005), astro-ph/0411468.
- [31] D. J. H. Chung and H. Yoo, *Phys. Rev. D* **87**, 023516 (2013), 1110.5931.
- [32] D. J. H. Chung, H. Yoo, and P. Zhou, *Phys. Rev. D* **91**, 043516 (2015), 1306.1966.
- [33] S. Ling and A. J. Long, *Phys. Rev. D* **103**, 103532 (2021), 2101.11621.
- [34] E. W. Kolb and A. J. Long (2023), 2312.09042.
- [35] P. W. Graham, J. Mardon, and S. Rajendran, *Physical Review D* **93** (2016), ISSN 2470-0029, URL <http://dx.doi.org/10.1103/PhysRevD.93.103520>.
- [36] D. J. H. Chung and A. Upadhye, *Phys. Rev. D* **95**, 023503 (2017), 1610.04284.
- [37] D. J. H. Chung and S. C. Tadepalli, *Phys. Rev. D* **109**, 023539 (2024), 2309.17010.
- [38] J. Martin and V. Vennin, *JCAP* **2018**, 063 (2018), 1801.09949.
- [39] T. Qiu, J. Evslin, Y.-F. Cai, M. Li, and X. Zhang, *Journal of Cosmology and Astroparticle Physics* **2011**, 036–036 (2011), ISSN 1475-7516, URL <http://dx.doi.org/10.1088/1475-7516/2011/10/036>.
- [40] Y.-F. Cai, D. A. Easson, and R. Brandenberger, *JCAP* **2012**, 020 (2012), 1206.2382.
- [41] D. J. Chung and A. Upadhye, *Physical Review D* **98** (2018), ISSN 2470-0029, URL <http://dx.doi.org/10.1103/PhysRevD.98.023525>.
- [42] J. Chluba and D. Grin, *Mon. Not. Roy. Astron. Soc.* **434**, 1619 (2013), 1304.4596.
- [43] S. Ando, N. Hiroshima, and K. Ishiwata, *Physical Review D* **106** (2022), ISSN 2470-0029, URL <http://dx.doi.org/10.1103/PhysRevD.106.103014>.
- [44] A. S. Josan and A. M. Green, *Physical Review D* **82** (2010), ISSN 1550-2368, 1006.4970, URL <http://dx.doi.org/10.1103/PhysRevD.82.083527>.
- [45] M. Karami, N. Afshordi, and J. Zavala, *Forward modelling of quasar light curves and the cosmological matter power spectrum on milliparsec scales* (2018), 1805.06984.
- [46] N. Afshordi, P. McDonald, and D. N. Spergel, *The Astrophysical Journal* **594**, L71–L74 (2003), ISSN 1538-4357, URL <http://dx.doi.org/10.1086/378763>.
- [47] I. Esteban, A. H. G. Peter, and S. Y. Kim, *Milky way satellite velocities reveal the dark matter power spectrum at small scales* (2023), 2306.04674.
- [48] A. Dekker and A. Kravtsov, *Constraints on blue and red tilted primordial power spectra using dwarf galaxy properties* (2024), 2407.04198, URL <https://arxiv.org/abs/2407.04198>.
- [49] D. J. H. Chung, M. Munchmeyer, and S. C. Tadepalli (2023), 2306.09456.
- [50] T. Sekiguchi, H. Tashiro, J. Silk, and N. Sugiyama, *Journal of Cosmology and Astroparticle Physics* **2014**, 001–001 (2014), ISSN 1475-7516, URL <http://dx.doi.org/10.1088/1475-7516/2014/03/001>.
- [51] J. R. Pritchard and A. Loeb, *Rept. Prog. Phys.* **75**, 086901 (2012), 1109.6012.
- [52] S. Furlanetto, S. P. Oh, and F. Briggs, *Phys. Rept.* **433**, 181 (2006), astro-ph/0608032.
- [53] M. Zaldarriaga, S. R. Furlanetto, and L. Hernquist, *Astrophys. J.* **608**, 622 (2004), astro-ph/0311514.
- [54] A. Loeb and M. Zaldarriaga, *Phys. Rev. Lett.* **92**, 211301 (2004), astro-ph/0312134.
- [55] M. Zaldarriaga, S. R. Furlanetto, and L. Hernquist, *The Astrophysical Journal* **608**, 622–635 (2004), ISSN 1538-4357, astro-ph/0311514, URL <http://dx.doi.org/10.1086/386327>.
- [56] A. Loeb and M. Zaldarriaga, *Physical Review Letters* **92** (2004), ISSN 1079-7114, astro-ph/0312134, URL <http://dx.doi.org/10.1103/PhysRevLett.92.211301>.
- [57] S. R. Furlanetto, *Monthly Notices of the Royal Astronomical Society* **371**, 867–878 (2006), ISSN 1365-2966, astro-ph/0604040, URL <http://dx.doi.org/10.1111/j.1365-2966.2006.10725.x>.
- [58] J. Silk, *Astrophys. J.* **151**, 459 (1968).
- [59] J. O. Burns et al., *Astrophys. J.* **844**, 33 (2017), 1704.02651.
- [60] J. O. Burns, S. Bale, and R. F. Bradley, in *American Astronomical Society Meeting Abstracts* (2019), vol. 234, p. 212.02.
- [61] J. Burns et al., in *Bulletin of the American Astronomical Society* (2019), vol. 51, p. 178, 1907.05407.
- [62] S. D. Bale et al. (2023), 2301.10345.
- [63] X. Chen et al., *Chinese Journal of Space Science* **43**, 43 (2023).
- [64] R. S. Polidan et al. (2024), 2404.03840.
- [65] T. J. W. Lazio et al. (2009), vol. 213 of *American Astronomical Society Meeting Abstracts*, p. 451.02.
- [66] D. C. Price et al., *Monthly Notices of the Royal Astronomical Society* (2018), ISSN 1365-2966, 1709.09313, URL <http://dx.doi.org/10.1093/mnras/sty1244>.
- [67] K. Artuc and E. d. L. Acedo (2024), 2406.10096.

- [68] H. T. J. Bevins et al., *Nature Astronomy* **6**, 1473–1483 (2022), ISSN 2397-3366, URL <http://dx.doi.org/10.1038/s41550-022-01825-6>.
- [69] T. Jishnu Nambissan et al., *Experimental Astronomy* **51**, 193 (2021).
- [70] S. Blyth et al. (2015), URL <https://api.semanticscholar.org/CorpusID:125493178>.
- [71] U. Maio, B. Ciardi, and L. V. E. Koopmans, *Bulk flows and end of the dark ages with the ska* (2015), 1501.04104, URL <https://arxiv.org/abs/1501.04104>.
- [72] R. A. Monsalve et al., *Monthly Notices of the Royal Astronomical Society* **530**, 4125–4147 (2024), ISSN 1365-2966, URL <http://dx.doi.org/10.1093/mnras/stae1138>.
- [73] D. Jones, S. Palatnick, R. Chen, A. Beane, and A. Lidz, *The Astrophysical Journal* **913**, 7 (2021), ISSN 1538-4357, 2101.07177, URL <http://dx.doi.org/10.3847/1538-4357/abf0a9>.
- [74] E. Vanzan, A. Raccanelli, and N. Bartolo, *JCAP* **03**, 001 (2024), 2306.09252.
- [75] S. C. Hotinli, D. J. E. Marsh, and M. Kamionkowski, *Phys. Rev. D* **106**, 043529 (2022), 2112.06943.
- [76] J. Flitter and E. D. Kovetz, *Phys. Rev. D* **106**, 063504 (2022), 2207.05083.
- [77] J. B. Muñoz, C. Dvorkin, and F.-Y. Cyr-Racine, *Physical Review D* **101** (2020), ISSN 2470-0029, 1911.11144, URL <http://dx.doi.org/10.1103/PhysRevD.101.063526>.
- [78] J. B. Muñoz, E. D. Kovetz, A. Raccanelli, M. Kamionkowski, and J. Silk, *JCAP* **2017**, 032 (2017), 1611.05883.
- [79] P. S. Cole and J. Silk, *Monthly Notices of the Royal Astronomical Society* **501**, 2627–2634 (2020), ISSN 1365-2966, 1912.02171, URL <http://dx.doi.org/10.1093/mnras/staa3638>.
- [80] K. Short, J. L. Bernal, K. K. Boddy, V. Gluscevic, and L. Verde, *Dark matter-baryon scattering effects on temperature perturbations and implications for cosmic dawn* (2022), 2203.16524.
- [81] T. Driskell et al., *Physical Review D* **106** (2022), ISSN 2470-0029, 2209.04499, URL <http://dx.doi.org/10.1103/PhysRevD.106.103525>.
- [82] Y. Ali-Haïmoud, P. D. Meerburg, and S. Yuan, *Phys. Rev. D* **89**, 083506 (2014), 1312.4948.
- [83] N. Bartolo, S. Matarrese, and A. Riotto, *Physical Review D* **64** (2001), ISSN 1089-4918, astro-ph/0107502, URL <http://dx.doi.org/10.1103/PhysRevD.64.123504>.
- [84] A. Linde and V. Mukhanov, *Physical Review D* **56**, R535–R539 (1997), ISSN 1089-4918, astro-ph/9610219, URL <http://dx.doi.org/10.1103/PhysRevD.56.R535>.
- [85] Y. Takeuchi and S. Chongchitnan, *Monthly Notices of the Royal Astronomical Society* **439**, 1125–1135 (2014), ISSN 0035-8711, 1311.2585, URL <http://dx.doi.org/10.1093/mnras/stu059>.
- [86] S. Ghosh, S. Kumar, and Y. Tsai, *Journal of Cosmology and Astroparticle Physics* **2022**, 014 (2022), ISSN 1475-7516, 2107.09076, URL <http://dx.doi.org/10.1088/1475-7516/2022/05/014>.
- [87] T. Minoda, S. Yoshiura, and T. Takahashi, *Physical Review D* **105** (2022), ISSN 2470-0029, 2112.15135, URL <http://dx.doi.org/10.1103/PhysRevD.105.083523>.
- [88] M. Kawasaki, T. Sekiguchi, and T. Takahashi, *Journal of Cosmology and Astroparticle Physics* **2011**, 028–028 (2011), ISSN 1475-7516, 1104.5591, URL <http://dx.doi.org/10.1088/1475-7516/2011/10/028>.
- [89] S. Kasuya and M. Kawasaki, *Physical Review D* **80** (2009), ISSN 1550-2368, 0904.3800, URL <http://dx.doi.org/10.1103/PhysRevD.80.023516>.
- [90] S. Kasuya, M. Kawasaki, and T. Yanagida, *Physics Letters B* **409**, 94 (1997), hep-ph/9608405.
- [91] D. Wands, N. Bartolo, S. Matarrese, and A. Riotto, *Physical Review D* **66** (2002), ISSN 1089-4918, astro-ph/0205253, URL <http://dx.doi.org/10.1103/PhysRevD.66.043520>.
- [92] D. J. Chung and S. C. Tadepalli, *Physical Review D* **105** (2022), ISSN 2470-0029, URL <http://dx.doi.org/10.1103/PhysRevD.105.123511>.
- [93] J. Hamann, S. Hannestad, G. G. Raffelt, and Y. Y. Y. Wong, *JCAP* **06**, 022 (2009), 0904.0647.
- [94] M. P. Hertzberg, M. Tegmark, and F. Wilczek, *Phys. Rev. D* **78**, 083507 (2008), 0807.1726.
- [95] D. J. E. Marsh, D. Grin, R. Hlozek, and P. G. Ferreira, *Phys. Rev. D* **87**, 121701 (2013), 1303.3008.
- [96] M. A. Amin and M. Mirbabayi, *A lower bound on dark matter mass* (2024), 2211.09775, URL <https://arxiv.org/abs/2211.09775>.
- [97] C. Caprini, R. Durrer, T. Konstandin, and G. Servant, *Phys. Rev. D* **79**, 083519 (2009), 0901.1661.
- [98] M. Gorghetto, E. Hardy, J. March-Russell, N. Song, and S. M. West, *Journal of Cosmology and Astroparticle Physics* **2022**, 018 (2022), ISSN 1475-7516, 2203.10100, URL <http://dx.doi.org/10.1088/1475-7516/2022/08/018>.
- [99] M. Redi and A. Tesi, *Phys. Rev. D* **107**, 095032 (2023), 2211.06421.
- [100] A. Kosowsky and M. S. Turner, *Physical Review D* **52**, R1739–R1743 (1995), ISSN 0556-2821, URL <http://dx.doi.org/10.1103/PhysRevD.52.R1739>.
- [101] D. Baumann et al., in *AIP Conference Proceedings* (AIP, 2009), URL <http://dx.doi.org/10.1063/1.3160885>.
- [102] G. Cabass, E. Di Valentino, A. Melchiorri, E. Pajer, and J. Silk, *Physical Review D* **94** (2016), ISSN 2470-0029, URL <http://dx.doi.org/10.1103/PhysRevD.94.023523>.
- [103] P. Adshead, R. Easther, J. Pritchard, and A. Loeb, *JCAP* **02**, 021 (2011), 1007.3748.
- [104] J. E. Lidsey, A. R. Liddle, E. W. Kolb, E. J. Copeland, T. Barreiro, and M. Abney, *Reviews of Modern Physics* **69**, 373–410 (1997), ISSN 1539-0756, astro-ph/9508078, URL <http://dx.doi.org/10.1103/RevModPhys.69.373>.
- [105] J.-O. Gong, *Journal of Cosmology and Astroparticle Physics* **2015**, 041–041 (2015), ISSN 1475-7516, 1409.8151, URL <http://dx.doi.org/10.1088/1475-7516/2015/05/041>.
- [106] S. Das and R. Ramos, *Universe* **9**, 76 (2023), ISSN 2218-1997, URL <http://dx.doi.org/10.3390/universe9020076>.
- [107] P. Madau, A. Meiksin, and M. J. Rees, *Astrophys. J.* **475**, 429 (1997), astro-ph/9608010.
- [108] J. R. Pritchard and A. Loeb, *Phys. Rev. D* **78**, 103511 (2008), 0802.2102.
- [109] J. R. Pritchard and A. Loeb, *Phys. Rev. D* **82**, 023006 (2010), 1005.4057.
- [110] S. R. Furlanetto (2019), 1909.12430.
- [111] A. Lewis and A. Challinor, *Phys. Rev. D* **76**, 083005 (2007), astro-ph/0702600.
- [112] S. Furlanetto et al. (2009), 0902.3259.
- [113] I. T. Iliev, P. R. Shapiro, A. Ferrara, and H. Martel,

- The Astrophysical Journal **572**, L123–L126 (2002), ISSN 1538-4357, astro-ph/0202410, URL <http://dx.doi.org/10.1086/341869>.
- [114] E. D. Kovetz et al. (2017), 1709.09066.
- [115] J. L. Bernal and E. D. Kovetz, *Astron. Astrophys. Rev.* **30**, 5 (2022), 2206.15377.
- [116] V. V. Sobolev, *Soviet Astronomy* **1**, 678 (1957).
- [117] K. Short, J. L. Bernal, A. Raccanelli, L. Verde, and J. Chluba, *JCAP* **07**, 020 (2020), 1912.07409.
- [118] S. Bharadwaj and S. S. Ali, *Mon. Not. Roy. Astron. Soc.* **352**, 142 (2004), astro-ph/0401206.
- [119] D. Blas, J. Lesgourgues, and T. Tram, *Journal of Cosmology and Astroparticle Physics* **2011**, 034–034 (2011), ISSN 1475-7516, URL <http://dx.doi.org/10.1088/1475-7516/2011/07/034>.
- [120] G. Scelfo, N. Bellomo, A. Raccanelli, S. Matarrese, and L. Verde, *JCAP* **09**, 039 (2018), 1809.03528.
- [121] M. Shiraishi, J. B. Muñoz, M. Kamionkowski, and A. Raccanelli, *Phys. Rev. D* **93**, 103506 (2016), 1603.01206.
- [122] J. B. Muñoz, Y. Ali-Haïmoud, and M. Kamionkowski, *Phys. Rev. D* **92**, 083508 (2015), 1506.04152.
- [123] A. Hall, C. Bonvin, and A. Challinor, *Phys. Rev. D* **87**, 064026 (2013), 1212.0728.
- [124] R. A. FISHER, *Annals of Eugenics* **6**, 391 (1935), <https://onlinelibrary.wiley.com/doi/pdf/10.1111/j.1469-1809.1935.tb02120.x>, URL <https://onlinelibrary.wiley.com/doi/abs/10.1111/j.1469-1809.1935.tb02120.x>.
- [125] D. Coe, *Fisher matrices and confidence ellipses: A quick-start guide and software* (2009), 0906.4123.
- [126] N. Bellomo, J. L. Bernal, G. Scelfo, A. Raccanelli, and L. Verde, *JCAP* **10**, 016 (2020), 2005.10384.
- [127] J. L. Bernal, N. Bellomo, A. Raccanelli, and L. Verde, *JCAP* **2020**, 017 (2020), 2005.09666.
- [128] L. Verde, *Statistical Methods in Cosmology* (Springer Berlin Heidelberg, 2010), p. 147–177, ISBN 9783642105982.
- [129] A. Heavens, *Statistical techniques in cosmology* (2010), 0906.0664, URL <https://arxiv.org/abs/0906.0664>.
- [130] M. Tegmark, A. N. Taylor, and A. F. Heavens, *The Astrophysical Journal* **480**, 22–35 (1997), ISSN 1538-4357, astro-ph/9603021, URL <http://dx.doi.org/10.1086/303939>.
- [131] M. S. Vogeley and A. S. Szalay, *The Astrophysical Journal* **465**, 34 (1996), ISSN 1538-4357, astro-ph/9601185, URL <http://dx.doi.org/10.1086/177399>.
- [132] M. Tegmark et al., *Physical Review D* **69** (2004), ISSN 1550-2368, astro-ph/0310723, URL <http://dx.doi.org/10.1103/PhysRevD.69.103501>.
- [133] H. Seo and D. J. Eisenstein, *The Astrophysical Journal* **598**, 720–740 (2003), ISSN 1538-4357, astro-ph/0307460, URL <http://dx.doi.org/10.1086/379122>.
- [134] A. Goel et al., *Probing the cosmic dark ages with the lunar crater radio telescope* (2022), 2205.05745, URL <https://arxiv.org/abs/2205.05745>.
- [135] A. Raccanelli, D. Bacon, J. de Kruijf, E. Vanzan, and F. Semenzato (in prep.).
- [136] S. Jester and H. Falcke, *New Astronomy Reviews* **53**, 1–26 (2009), ISSN 1387-6473, 0902.0493, URL <http://dx.doi.org/10.1016/j.newar.2009.02.001>.
- [137] A. Datta et al., *Effects of the ionosphere on ground-based detection of the global 21 cm signal from the cosmic dawn and the dark ages* (2016), 1409.0513, URL <https://arxiv.org/abs/1409.0513>.
- [138] L. V. E. Koopmans et al., *Experimental Astronomy* **51**, 1641 (2021), 1908.04296.